



# SIMULATION OF A DEPLOYABLE TENSEGRITY COLUMN BASED ON THE FINITE ELEMENT MODELING AND MULTIBODY DYNAMICS SIMULATIONS

A. AL SABOUNI-ZAWADZKA<sup>1</sup>, A. ZAWADZKI<sup>2</sup>

The present paper is dedicated to the analysis of deployable tensegrity columns. The main aim of this work is to present a technique, developed by combining the finite element (FE) analysis and the multibody dynamics (MBD) simulation, which enables precise and reliable simulations of deployable structures. While the finite element model of the column provides information on structural behavior in the deployed state, the dynamical modeling allows to analyze various deployment scenarios, choose active cables for the deployment and for the self-stress application, and to control distributions of internal forces during the assembly process. An example of a deployable column based on a popular tensegrity module – a 3-strut simplex – is presented. By analyzing the proposed column with the use of the developed method it is proven that the technique is suitable for complex simulations of deployable systems.

*Keywords:* deployable structures, tensegrity, finite element modeling, multibody dynamics

<sup>1</sup> Ph.D., Eng., Warsaw University of Technology, Faculty of Civil Engineering, Al. Armii Ludowej 16, 00-637 Warsaw, Poland, e-mail: a.sabouni@il.pw.edu.pl

<sup>2</sup> Ph.D., Eng., Warsaw University of Technology, Faculty of Automotive and Construction Machinery Engineering, Narbutta 84, 02-524 Warsaw, Poland, e-mail: adam.zawadzki@pw.edu.pl

## 1. INTRODUCTION

In recent years, a progressive development of deployable structures has been observed. Such structures, also known as expandable, erectable or developable systems, are transported in a stowed form and deployed at the place of use. They must be designed specifically for large, autonomous geometry changes, as they are expanded, usually automatically, from the folded form to the required service configuration.

Deployable structures are applied both in space and on Earth, where they are eagerly used by architects as well as civil engineers. They are commonly used as temporary and emergency structures, as they can be quickly erected and disassembled when no longer needed. The structures aimed at space applications, such as masts, solar arrays or antennas, should be very compact when stowed and must be designed for automatic expansion in space. Some of the developed structural concepts and technology needs for large space systems are presented in [1, 2]. Deployable structures for earthly applications do not have to meet the same criteria as in space, as they are used in a completely different environment. However, some of the requirements remain – they should also have a compact stowed form and they should be deployed automatically or with a limited contribution of a human. In [3] a portable scissor bridge is presented, which is used in emergency situations to access remote locations affected by a disaster. A concept of lightweight tensegrity structures, that can be used as deployable wide span roofs, temporary buildings or bridges, is discussed in [4].

One of the most important features of deployable systems is their stiffness-to-mass ratio. They are usually very lightweight structures with a relatively high load-bearing capacity. Moreover, they can be easily transported due to the compact stowed form, and deployed even to very large sizes depending on the application. The crucial aspect of the design of such systems is to find a proper balance between the dimensions of the folded structure and the required form and load-carrying capacity of the erected one. Therefore, not every structural system is suitable for the deployment. Among the structures commonly used in such applications, tensegrity systems [5-7] deserve special attention.

The word “tensegrity” was created by Buckminster Fuller who combined two terms “tension” and “integrity” [8]. Various definitions of tensegrity can be found in the literature [5-8]. Fuller defined a tensegrity structure as “an assemblage of tension and compression components arranged in a discontinuous compression system” [8]. Tensegrity systems have many interesting properties that arise from the occurrence of infinitesimal mechanisms, which are balanced with self-equilibrating

sets of forces, called self-stress states. Such forces depend neither on the outer loads nor on the applied boundary conditions. Tensegrity structures are lightweight, they have advantageous stiffness-to-mass ratio and may be used in adaptive systems. Their behavior can be controlled and adjusted by changing the values of self-stress forces.

In [9] inherent properties of tensegrity, which allow to regard them as smart structures, are described. These are: self-control, self-diagnosis, self-repair and self-adjustment. The mentioned features are very important in the deployable applications, especially the ability of self-stiffening under the external load and the possibility of active control through the adjustment of prestressing forces [9]. What is important, the stiffness of the structure can be controlled by changing the forces only in selected active cables, which allows the designers to reduce the number of actuators. Also the deployment of the structure can be performed using some active elements, which can (but not necessarily) be the same cables that are used for structural control.

Several works on deployable tensegrity structures can be found in the literature. A group of scientists from the Swiss Federal Institute of Technology in Lausanne (EPFL) developed a prototype of a deployable tensegrity footbridge. The structure described in [10-12] consists of four pentagonal tensegrity modules, which together span a distance of 16 m. Tibert, in his doctoral thesis [13], presents a concept of a deployable tensegrity mast that was inspired by the structure proposed by Snelson in his patent from 1965 [14]. The mast is constructed using 3-strut simplex modules with an overlap. Tibert [13] tested various deployment schemes and analyzed mechanical behavior of the structure. A similar structure is described in [15], where an algorithm for the reconfiguration of a two-stage tensegrity mast is proposed.

In the present paper, a deployable tensegrity column is proposed. The main aim of this work is to present a technique developed by the authors, that can be used for analysis of adaptive tensegrity columns. The described method is based on the combination of the finite element (FE) analysis and the multibody dynamics (MBD) simulation. While the finite element model of the column provides information on structural behavior in the deployed state, the dynamical modeling allows to analyze various deployment scenarios, choose active cables for the deployment and for the self-stress application, and to control distributions of internal forces during the assembly process. The FE analysis was performed in SOFiSTiK software, using the geometrically non-linear analysis. The MBD simulations were made in MSC ADAMS using dynamical systems analysis described in detail further.

The structures considered in this paper are three variants of a tensegrity column that is based on a 3-strut simplex module. The developed approach allowed the authors to analyze various

deployment scenarios of the column, including an original scenario which has not yet been presented in the literature. This innovative deployment scheme turned out to be most efficient and it assured the best stability of the structure during the erection.

The proposed column can be used as a support of temporary structures, such as lightweight ceilings, large scale tents, etc. It is also aimed at emergency applications, for example as an additional support of the structure in case of its partial damage or in the endangered buildings to prevent their abrupt collapse. Among possible applications of such structures one should also mention: areas affected by the earthquakes, places in the structures which are difficult to access, historic buildings where it is impossible to construct typical heavy supports. In the presented analyses it is assumed that the loads from the supported structure are transferred to the nodes of the upper surface of the column in the form of three concentrated forces acting vertically.

## 2. SYNERGY OF FE MODELING AND MBD SIMULATION

Finite element modeling enables qualitative and quantitative analyses of the behavior of deformable structures with the defined boundary conditions and loading. It takes into account structural shape changes during the simulations. Multibody dynamics simulation, on the other hand, enables fast simulations of the systems consisting of rigid bodies with any translational or rotational displacements. It does not consider deformations of structural members, since its equations of motion are built for rigid bodies, applied forces and physical constraints. The combined use of MBD and FE analysis creates synergy that results in precise and reliable simulations of complicated structural systems in motion.

During the process of erecting a temporary column, the following computations and activities typical for FE modeling and MBD simulations are intertwined and supplemented.

FE-1: Final form finding of tensegrity configurations is performed. Geometry and self-stress parameters are defined.

MBD-1: Struts and cables lie in the initial position (on top or next to each other). The following parameters are defined: active structural members, friction between the elements, etc.

MBD-2: Modules (individual or in groups) approach the required configuration. Realization of the requested form is achieved by changing the length of active cables.

FE-2: The found final configuration can be checked and analysis of displacements and stresses can be performed.

FE-3: The range of prestressing forces can be determined so that the load-carrying capacity of individual structural members is not exceeded.

MBD-3: The prestressed structure stands and is ready to carry temporary loads.

FE-4: The structure works under the applied loads. Additional prestressing forces appear in cables, which stiffen the column [9]. Displacement and stresses can be calculated at any loading conditions, within the determined range of self-stress, in order to prevent the excessive deformation or structural damage.

### 3. FE MODELING OF THE COLUMN

Finite element model of a cable-strut structure with self-stress included is based on the geometrically nonlinear theory [16]. Incremental formulation can be expressed in the form

$$(3.1) \quad \mathbf{K}_T(\mathbf{q})\Delta\mathbf{q} = \Delta\mathbf{Q},$$

$$(3.2) \quad \mathbf{K}_T(\mathbf{q}) = \mathbf{K}_L + (S_0 + \Delta N)\mathbf{K}_G + \mathbf{K}_{NL}(\mathbf{q}),$$

where:

$\mathbf{q}$  - vector of nodal displacements,  $\Delta\mathbf{q}$  - increment of nodal displacement vector,  $\mathbf{K}_T$  - tangential stiffness matrix,  $\Delta\mathbf{Q}$  - increment on load vector, based on external loads and normal forces with the influence of geometrical changes of cables and struts,  $\mathbf{K}_L$  - linear stiffness matrix,  $\mathbf{K}_G$  - geometric stiffness matrix,  $\mathbf{K}_{NL}(\mathbf{q})$  - symmetric displacement stiffness matrix,  $S_0$  - multiplier of initial self-stress,  $\Delta N$  - increment of  $S_0$  due to external loads.

Distribution of self-equilibrated normal forces to define the geometric stiffness matrix can be obtained by any method described in the literature [17, 18]. In the present paper a method based on the spectral analysis of the stiffness matrix is applied. SOFiSTiK software supported by programming in the Wolfram Mathematica environment is used for calculations.

The structure proposed in this paper is a deployable column based on a popular tensegrity module – a 3-strut simplex (Figure 1). It is a cable-strut structure obtained from a regular prism through the rotation of its lower or upper base by 150 degrees clockwise or counter-clockwise. The single module has one infinitesimal mechanism and one corresponding self-stress state, which is represented by the relative forces in structural members multiplied by the factor  $S_0$ . This factor is used further to express the level of self-stress.

In the analyzed structure three configurations of the module were used: standard, high and low (Figure 2). The geometric parameters as well as the self-stress values for the considered modules are given in Tables 1-2. The positive values of prestressing forces are assumed in the cables (elements in tension) and negative in struts (elements in compression).

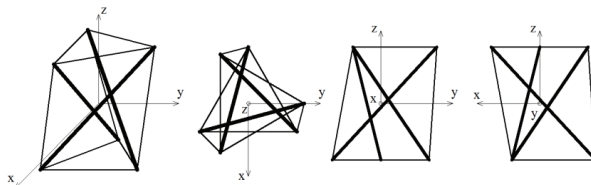


Fig. 1. Geometry of the standard 3-strut simplex module – axonometry and three views

Table 1. Geometric parameters of three simplex modules

		<b>standard</b>	<b>high</b>	<b>low</b>
height [m]		1.000	1.150	0.750
cable length [m]	bottom triangle	0.866	0.866	0.866
	top triangle	0.866	0.530	1.230
	diagonal	1.033	1.184	0.838
strut length [m]		1.390	1.390	1.390

Table 2. Self-stress states in three simplex modules

		<b>standard</b>	<b>high</b>	<b>low</b>
cables	bottom triangle	$0.154300 \cdot S_0$	$0.092145 \cdot S_0$	$0.222759 \cdot S_0$
	top triangle	$0.154300 \cdot S_0$	$0.150562 \cdot S_0$	$0.156846 \cdot S_0$
	diagonal	$0.318778 \cdot S_0$	$0.356449 \cdot S_0$	$0.262776 \cdot S_0$
struts		$-0.429065 \cdot S_0$	$-0.418469 \cdot S_0$	$-0.435974 \cdot S_0$

The analyzed column consists of four 3-strut simplex modules, connected in the nodes via mutual cables of their bases. The modules rotated clockwise and counter-clockwise are arranged alternately.

Three configurations of the column were considered (Figure 2):

- standard – a 4.00 m high column, consisting of four standard simplex modules;
- high – a 4.15 m high column, consisting of three standard simplex modules and one high module;
- low – a 3.75 m high column, consisting of three standard simplex modules and one low module.

The described configurations are three variants of the same column, as the upper module can be deployed to different heights depending on the considered use. All simplex modules have struts of

the same length and the height adjustment is performed by changing the lengths of the cables (see Table 1). In the considered case, a reasonable range of the height adjustment (taking into account forces in structural members and practical aspects of deployment) is 4.00 m +0.15 m/-0.25 m.

The columns consisting of four modules have four possible self-stress states. In the present study, a uniform state of prestressing forces was adopted – the same values of  $S_0$  were introduced to all modules. The columns were supported in three bottom nodes and loaded with three concentrated forces  $P=8.33$  kN applied to the upper nodes of the structures. The adopted load corresponds to the uniformly distributed surface load  $q=1$  kN/m<sup>2</sup> acting on the area of 25 m<sup>2</sup>. Additionally, the self-weight of structural members was considered. The load and self-stress values were adopted so that the forces in cables and struts do not exceed 90 % of the maximum load specified below. In the analyzed structures, typical elements taken from the available systems were used. The following cross sections were applied:

- cables –  $\phi=10.0$  mm made of steel SC460 – maximum load  $N_{Rd}=71.1$  kN,
- struts – hollow cross-section  $\phi=54.0$  mm, wall thickness 2.6 mm, made of steel S355J2 – maximum load  $N_{Rd}=84$  kN.

The columns were analyzed in SOFiSTiK software [19], using the finite element method (FEM) within the geometrically non-linear theory that takes into account the effects of the geometrical system modification and includes the second-order theory (to consider the effect of self-stress). It should be noted, that depending on the geometry and elastic properties of the simplex module, various responses (from a module with struts locking to a fully foldable structure) and various failure modes (rapture of triangle cables, slack of diagonal cables or buckling of the struts) may be obtained during the uniaxial compression.

In the performed analyses three parameters were measured: vertical displacement of the upper node (see Figure 2), maximum tensile force in the cable and compressive force in the strut (elements with maximum forces are marked with red lines in Figure 2).

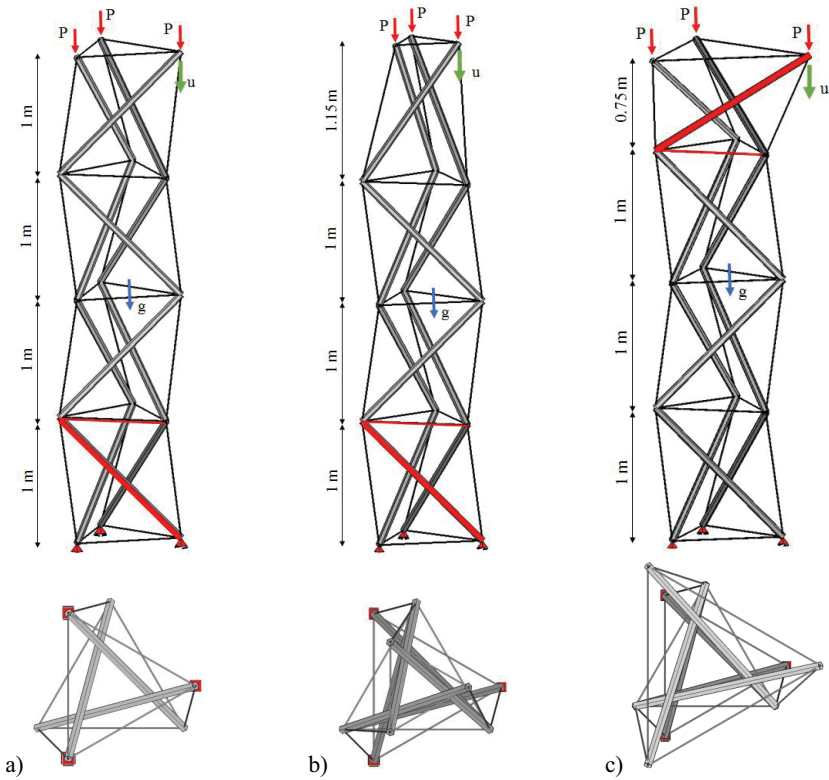


Fig. 2. Configurations of the column: a) standard column; b) high column; c) low column

Figure 3 shows how the considered columns deflect (on the top) under the given load  $3 \cdot P = 25$  kN, depending on the applied prestressing forces. The displacement was obtained numerically for selected values of the factor  $S_0$  and then approximated with a curve. It can be noticed that the displacement of the upper surface of the structure can be reduced by  $\sim 50\%$ , only by increasing the level of self-stress from 1 kN to 120 kN. When the column is deployed to a smaller height, considerably bigger values of deflections are obtained. In the high configuration, on the other hand, the deflections reach smaller values. This should be taken into account while designing the initial configuration of the structure.

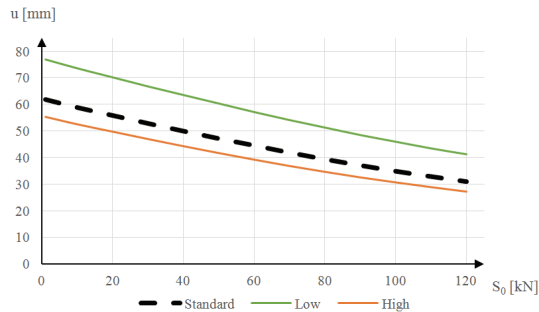


Fig. 3. Influence of self-stress on the displacement of the upper surface node

The diagrams of maximum tensile and compressive forces in structural members are presented in Figure 4. The forces, similarly to displacements, were obtained numerically for selected values of the factor  $S_0$  and then approximated with curves. It should be taken into account that the biggest values of the considered forces are reached in elements of the bottom module in the standard and high column, and in the top module of the low column (see red lines in Figure 2). Therefore, the curves in Figures 4a and 4b represent forces in two different cables and two different struts.

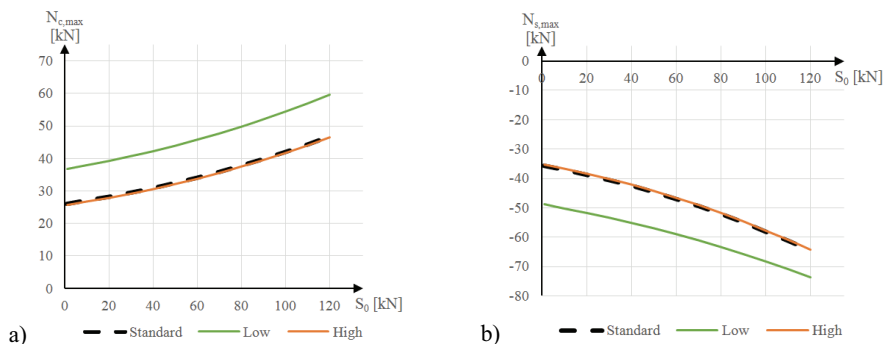


Fig. 4. Influence of self-stress on: a) maximum tensile force in cables; b) maximum compressive force in struts

It may be noticed that the deployment of the column to a bigger height does not change the maximum values of the forces in structural elements. In the high column, the biggest forces occur in the same elements as in the standard one and, what is more, the values of these forces remain unchanged. When the column is deployed to a smaller height, the forces increase significantly. This

effect must be considered in the design process, as there is a risk of exceeding the load-bearing capacity of structural members with too high values of the applied self-stress.

#### 4. MBD SIMULATIONS

MSC ADAMS/View was chosen to perform dynamic analyses of the considered deployable systems. This software had not been used much for simulations of spatial structures with self-stress; only a few papers dealing with single tensegrity modules can be found [20, 21]. Therefore, parallel or prior to simulations the authors verified the software by comparing selected results with the ones obtained from FE analysis.

In this paper, two deployment patterns of tensegrity columns described in the previous section were analyzed (Figure 5), in order to establish how many and which cables need to be controlled during the deployment and height adjustment.

The first one is a classical, most intuitive version, described in detail e.g. by Tibert [13]. One of the column's bases lays on an even surface, the gravity force acts perpendicular to this surface, so the mass forces act in the direction of the column's axis the whole time. It will be referred in this paper as an A-pattern. The second one assumes preliminary assembly of individual modules in the horizontal position and then a module-after-module deployment. It will be referred in this paper as a B-pattern. In this pattern the system becomes a tensegrity column in the last phase of deployment, when the active cables finish the movement (Figure 5b – in the lower right corner).



Fig. 5. Deployment patterns: a) A-pattern; b) B-pattern

All the simulations assume movement in the gravity field and, after the deployment process, influence of external forces on structural elements. Mechanical properties i.e. masses and moments of inertia of elements are the same as in the FE computations. In the case of the struts, it is a straightforward relation, but cables were modeled in a specific way. Each cable consists of two bar members with the sum of masses and moments of inertia equal to the ones of a single steel cable. These bars are connected via a spring-damper element and a motion constraint (Figure 6). Each

section is connected with another one and with the struts using a ball-and-socket joint. Such a configuration enables the self-stress application using a spring's preload and the deploying motion using a motion constraint. It should be noted that the proposed MBD model enables the introduction of increased friction at the end joints and increased cable damping caused by self-stress. However, these effects are not included at this stage, as they require some additional parameters taken for example from the laboratory tests.

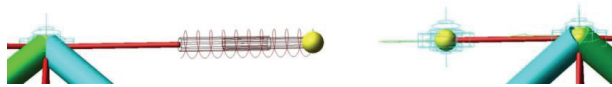


Fig. 6. Representation of a cable in dynamic simulations

The change of length is imposed only on the cables; there is no manipulation with the struts' lengths. Struts and cable modules are connected with each other using ball-and-socket joints. Moreover, nodes of the bottom base are connected with the ground in a way that corresponds to the support system applied in the FE models. Each tip of an element is ended with a ball of a negligible mass of  $10^{-4}$  kg (yellow pieces in figures) to assure a more flexible model manipulation throughout the analyzed scenarios. The same elements are used to model the cable behavior – the ball elements are connected by ball-and-socket joints, so when no force is transmitted through the cable it stays loose.

The performed simulations aimed at calculating dynamic forces acting on the structural members during the deployment. Each case was repeated for three different process times: 50, 100, 200 seconds to establish if it has any influence on the results. It was assumed that shorter time periods would be difficult to realize in real applications due to performance limitations of small actuators that need to be used to control the lengths of the cables. Moreover, it was assumed that the lengths of the struts stay constant as opposed to some research papers [22, 23]. Such an assumption was made because it ensures a correct force distribution throughout the structure to sustain its form and to be a tensegrity-class object. By designing a proper control strategy for manipulation of the cables' lengths, such a condition is fulfilled. The starting point for the simulations was to find the static equilibrium of the system, afterwards the simulation started what eliminated the initial system oscillations. All the simulations were performed using the basic solver "GSTIFF" integrator that uses backward differentiation methods and fixed coefficients for prediction and correlation, and using the basic formulation "I3" for the corrections of the computed integration error of the solution [24].

It was assumed that the deployment process consists of the following phases:

- A-pattern:

Phase 1. The structure lays folded vertically on the ground.

Phase 2. It deploys according to a specific algorithm that controls horizontal cables' lengths.

Phase 3. The top module adjusts its height to assure the desired pressure on the supported object.

Phase 4. The movement mechanisms are locked (in the physical application).

- B-pattern (Figures 7-8):

Phase 1. The structure lays folded horizontally on the ground.

Phase 2. Individual modules are prestressed to attain a tensegrity form.

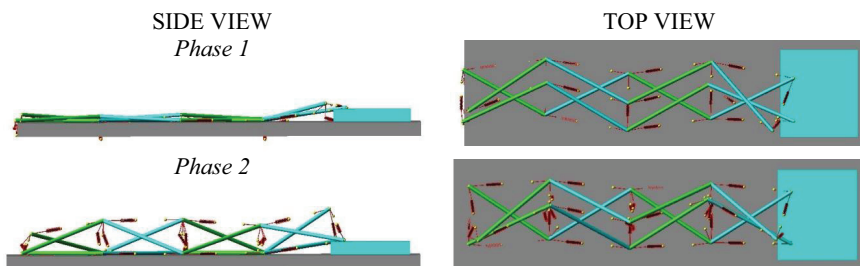
Phase 3. The system deploys module after module starting from the bottom or raising all the modules simultaneously to avoid friction against the ground (this scenario is shown in this paper).

Phase 4. The top module adjusts its height to assure the desired pressure on the supported object.

Phase 5. The movement mechanisms are locked (in the physical application).

The simulations were performed in such a manner that the structure was set in its standard working position, then it was loosen to establish its most natural form when unstressed (which is meant to be the initial shape for deployment).

Both deployment patterns were analyzed in terms of stability. The stability shall be understood as an ability to remain in any geometrical configuration during the deployment when the movement of active elements stops; or as an ability to change the geometry in a predicted manner when the movement continues. The A-pattern showed very unstable behavior during the deployment. Various possibilities of controlling the lengths of the cables were investigated and they all pointed at poor stability and susceptibility to even small external disturbances. The B-pattern turned out to be stable at all deployment phases thanks to the adopted division on: deployment and prestressing of the individual modules, deployment of the structure to the vertical position.



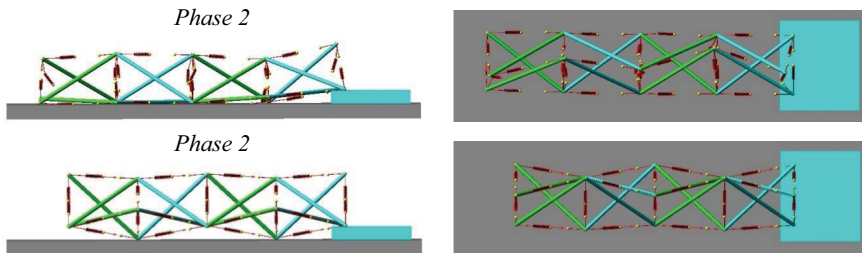


Fig. 7. Selected deployment phases of the column laying horizontally – phase 1 and 2 of B-pattern

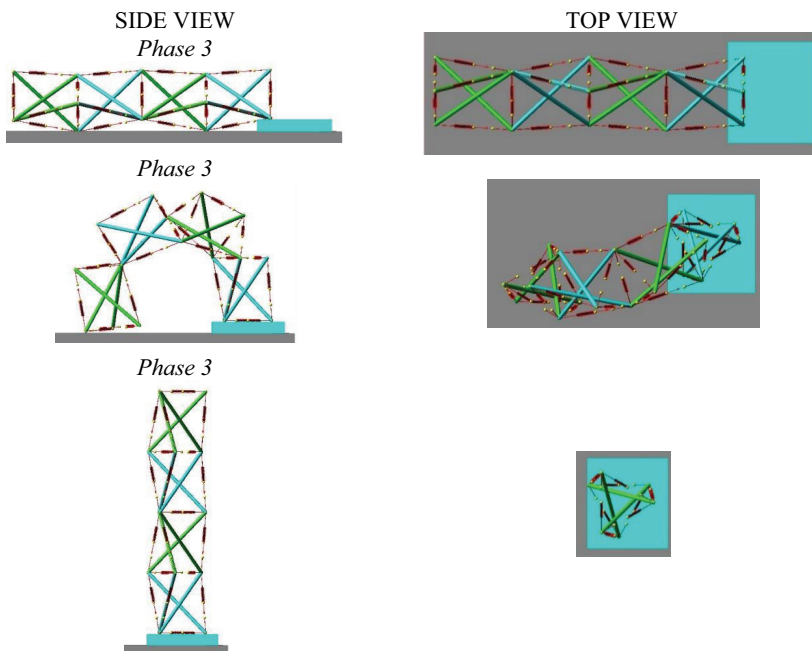


Fig. 8. Selected deployment phases of the column – phase 3 of B-pattern

In further analysis the B-pattern is considered. Figure 9a shows distributions of the forces in all cables for the second phase of deployment. It should be noted that although the cables are in tension, the forces are marked as negative – it results from the specific way of modeling tensegrity structures in ADAMS, where cables are modeled as prestressed springs.

The plot (Figure 9a) consists of two parts: disassembly and assembly. At the beginning of the simulation the modules of the column are prestressed with forces that assure the tensegrity form (derived from previous FE simulations). These modules are connected at bases. At time period  $0 \div 9$

seconds the internal forces decrease with elongation of the active cables. At time period 9÷30 seconds the structure lays relaxed on the ground, only the struts move on each other to find a stable static configuration. The assembly starts in the 30th second of the simulation. At time period 32÷37 seconds due to the contact forces between the struts, the forces oscillate and even change their sign to positive values. This happens because the fragments of the relaxed cables might be compressed in some transient configurations due to the inertia forces acting on the springs at which the forces are measured (see Figure 6). After 37th second the contact disappears and so do the oscillations. At time period 37÷54 seconds the forces are very small (but not zero) compared to prestress values what results from low mass of the entire structure. After 54th second the structure becomes stiffer with increasing prestress until it becomes its final tensegrity geometry. At the end of the simulation of the phase 2 values of the forces are equal to the values at the beginning of the simulation of the phase 3 (Figure 9b).

The trend of force transition at the beginning and at the end of the simulation results directly from the input function. At the beginning the movement accelerates, then it continues at constant speed to decelerate to zero at the end [24].

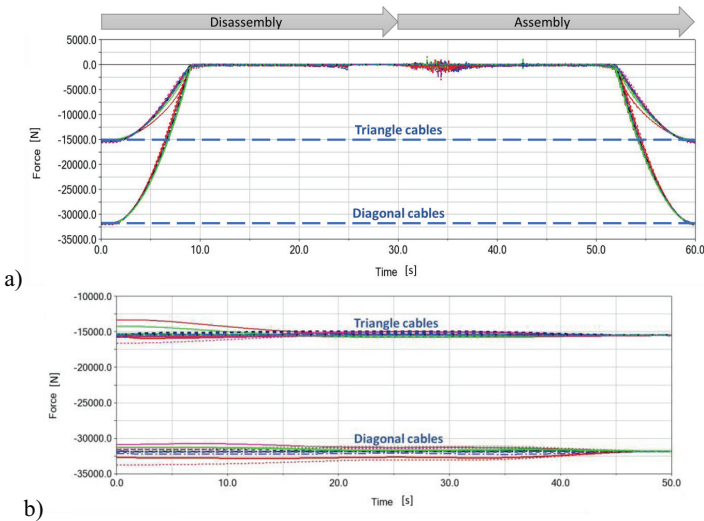


Fig. 9. Internal forces in all the cables during the deployment of the B-pattern column: a) phase 2; b) phase 3

It can be noticed in Figure 9b that individual initial forces differ from the values at the end of the simulation, what is caused mainly by the change of the gravity force vector direction relatively to the structure. The beginning of this simulation is the end of the phase 2 simulation described above.

The forces in all cables are given in Figure 9b and they differ within both groups – triangle cables and diagonal cables. The deviation can be explained on an example of one module. When the structure is set horizontally, the top cables transfer more force than the bottom ones due to the force distribution caused by the masses of elements (see Figure 8 first line). During the simulation time 0÷50 seconds these differences in forces decrease with obtaining a fully erected position. At the end of the simulation all the forces converge to the values characteristic to simplex modules.

Throughout the simulations, for aforementioned mass properties, the influence of the deployment time on internal forces was negligible in the case of the B-pattern column and hence only one run is described – 60 seconds for the 2nd phase and 50 seconds for the 3rd phase.

This deployment pattern is possible only when the second step is performed in such a way that all side cables' lengths are changed. If only one or two side cables are manipulated, the third one limits the struts movement. This effect could be eliminated by changing the lengths of base cables but it leads to an even more complicated physical realization, what was the reason for abandoning this approach. In the horizontal initial configuration, changing only the lengths of the base cables would lead to a similar effect but the physical realization would be more complicated, because then 15 instead of 12 cable actuators would have to be installed.

## 5. CONCLUSIONS

The present paper is an approach to the analysis of deployable tensegrity structures by combining the finite element (FE) modeling and multibody dynamics (MBD) simulations. The proposed approach is applied for a temporary deployable column based on the 3-strut simplex modules. The finite element model of the column is used for the final form-finding of the system, it also provides information on structural behavior in the deployed state. The dynamical modeling is used to analyze various deployment scenarios, choose active cables for the deployment and for the self-stress application, and to control distributions of internal forces during the assembly process. The proposed combination of MBD and FE analysis creates synergy that results in precise and reliable simulations of complex structural systems, such as the considered deployable tensegrity structures.

With the use of the described technique it is possible to investigate various possibilities of changing the geometry and physical properties of tensegrity structures. The performed simulations reflect the behavior of these structures both qualitatively and quantitatively.

Two deployment schemes were analyzed using the proposed method. The analyses of the B-pattern tensegrity column – the one that assumes preliminary assembly of individual modules in a horizontal position and then a module-after-module deployment – gave promising results from the point of view of future physical realization. The system can be built using the commonly available materials and actuators and that will be the next step for the authors.

Moreover, the performed simulations – the ones shown in this paper as well as other carried out by the authors – proved that the proposed technique is time- and cost-efficient. It has the potential to be used in the analysis of complex tensegrity systems both during the deployment phase and in the deployed state, with no need to carry out expensive and time consuming laboratory tests. It should be considered as a method aimed at preliminary investigations of the designed structures, which can indicate structural configurations, deployment schemes, active cables, etc., that should be afterwards tested in laboratory. This qualifies the proposed technique as a good tool for the analysis of deployable tensegrity structures.

*Acknowledgements:* Calculations using MSC ADAMS software were carried out at the Academic Computer Centre in Gdańsk.

## REFERENCES

1. Mikulas, M. M.; Thomson, M. State of the art and technology needs for large space structures. In *New and Projected Aeronautical and Space Systems, Design Concepts, and Loads: Flight-Vehicle Materials, Structures, and Dynamics*, ASME, New York, 1994, pp. 173–238.
2. Kiper, G.; Soylemez, E. Deployable space structures. 4th Int. Conf. on Recent Advances in Space Technologies, 2009, pp. 131-138.
3. Biro, M.; Bakar, N. Design and Analysis of Collapsible Scissor Bridge. MATEC Web of Conf., 2018.
4. Luchsinger, R.; Pedretti, A.; Steingruber, P.; Pedretti, M. *Light Weight Structures With Tensairity*, 2004.
5. Skelton, R.E.; de Oliveira, M.C. *Tensegrity Systems*, Springer, Dordrecht, Heidelberg, London, New York, 2009.
6. Motro, R. *Tensegrity: Structural Systems for the Future*, Kogan Page Science, London, 2003.
7. Gilewski, W.; Al Sabouni-Zawadzka, A. On possible applications of smart structures controlled by self-stress. *Archives of Civil and Mechanical Engineering*, 15, 2015, pp. 469-478.
8. Fuller, R. B. Tensile-integrity structures. US Patent 3,063,521,1962. Filed 31 August 1959, Granted 13 November 1962.
9. Al Sabouni-Zawadzka, A.; Gilewski, W. Inherent properties of smart tensegrity structures. *Applied Sciences*, 8 (5), 787, 2018.
10. Korkmaz, S.; Bel Hadj Ali, N.; Smith, I.F.C. Self-repair of a tensegrity pedestrian bridge through grouped actuation. *Proceedings of the International Conference on Computing in Civil and Building Engineering*, 2010.
11. Rhode-Barbarigos, L. *An Active Deployable Tensegrity Structure*. Ph. D. Thesis, 2012.
12. Rhode-Barbarigos, L.; Bel Hadj Ali, N.; Motro, R.; Smith, I.F.C. Designing tensegrity modules for pedestrian bridges. *Engineering Structures*, 32(4), 2010, pp. 1158-1167.
13. Tibert, G. *Deployable Tensegrity Structures for Space Applications*. Ph. D. Thesis, 2002.
14. Snelson, K. D. Continuous tension, discontinuous compression structures. US Patent 3,169,611, 1965. Filed 14 March 1960, Granted 16 February 1965.

15. González, A.; Luo, A.; Shia, D. Reconfiguration of multi-stage tensegrity structures using infinitesimal mechanisms. *Latin American Journal of Solids and Structures*, 16(3), 2019.
16. Crisfield, M.A. *Non-linear finite element analysis of solids and structures: Essentials*, John Wiley & Sons, New York, USA, 1991.
17. Juan, S.H.; Mirats Tur, J.M. Tensegrity frameworks. Static analysis review. *Mechanism and Machine Theory*, 43, 7, 2008, pp. 859–881.
18. Tibert, A.G.; Pellegrino, S. Review of Form-finding Methods for Tensegrity Structures. *International Journal of Solids and Structures*, 18, 4, 2003, pp. 209–223.
19. User guide, SOFiSTiK AG, Oberschleissheim, 2011.
20. Luo, A.; Wang, J.; Liu, H. Four-bar tensegrity robot based on ADAMS simulation. *IEEE International Conference on Mechatronics and Automation (ICMA)*, Takamatsu, 2017, pp. 1463-1468.
21. Mirats-Tur, J.; Camps, J. A three-DoF actuated robot. *Robotics & Automation Magazine, IEEE*, 2011.
22. Bruce, J.; Caluwaerts, K.; Iscen, A.; Sabelhaus, A.; Sunspir, V. Design and Evolution of a Modular Tensegrity Robot Platform. *IEEE International Conference on Mechatronics and Automation (ICMA)*, 2014.
23. Kim, K.; Chen, L.H.; Cera, B.; Daly, M.; Zhu, E.; Despois, J.; Agogino, A.; Sunspir, V.; Agogino, A. Hopping and rolling locomotion with spherical tensegrity robots, *2016 IEEE/RSJ International Conference on Intelligent Robots and Systems (IROS)*, Daejeon, 2016, pp. 4369-4376.
24. User guide, Using the Adams/View, MSC Software, 2010.

#### LIST OF FIGURES AND TABLES:

Fig. 1. Geometry of a 3-strut simplex module – axonometry and three views.

Rys. 1. Geometria modułu *simplex* 3-zastrzałowego – aksonometria i trzy rzuty.

Fig. 2. Configurations of the column: a) standard column; b) high column; c) low column.

Rys. 2. Konfiguracje słupów: a) podstawowa ; b) wysoka; c) niska.

Fig. 3. Influence of self-stress on the displacement of the upper surface node.

Rys. 3. Wpływ samonapężenia na przemieszczenie węzła na górnej płaszczyźnie.

Fig. 4. Influence of self-stress on: a) maximum tensile force in cables; b) maximum compressive force in struts.

Rys. 4. Wpływ samonapężenia na: a) maksymalną siłę rozciągającą w cięgnach; b) maksymalną siłę ściskającą w zastrzałach.

Fig. 5. Deployment patterns: a) A-pattern A; b) B-pattern B.

Rys. 5. Schematy rozwijania: a) schemat A; b) schemat B.

Fig. 6. Representation of a cable in dynamic simulations.

Fig. 6. Model cięgna do symulacji dynamicznych.

Fig. 7. Selected deployment phases of the column laying horizontally – phase 1 and 2 of B-pattern.

Rys. 7. Wybrane fazy rozwijania słupa spoczywającego poziomo – faza 1 i faza 2 ze schematu B.

Fig. 8. Selected deployment phases of the column – phase 3 of B-pattern.

Rys. 8. Wybrane fazy rozwijania słupa – faza 3 ze schematu B.

Fig. 9. Internal forces in all the cables during the deployment of the B-pattern column: a) phase 2; b) phase 3.

Rys. 9. Siły wewnętrzne we wszystkich cięgnach podczas rozwijania słupa ze schematu B: a) faza 2; b) faza 3.

Tab. 1. Geometric parameters of three simplex modules.

Tab. 1. Parametry geometryczne trzech wersji modułu *simplex*.

Tab. 2. Self-stress states in three simplex modules.

Tab. 2. Stany samonapężenia w trzech wersjach modułu *simplex*.

### SYMULACJA ROZWIJALNEGO SŁUPA TENSEGRITY

#### W OPARCIU O METODĘ ELEMENTÓW SKOŃCZONYCH I DYNAMIKĘ UKŁADÓW WIELOCZŁONOWYCH

*Słowa kluczowe:* struktury rozwijalne, tensegrity, metoda elementów skończonych, dynamika układów wieloczłonowych

#### PODSUMOWANIE:

W pracy został poruszony problem analizy rozwijalnych słupów tensegrity. Głównym celem opracowania jest zaprezentowanie techniki pozwalającej na zapewnienie niezawodnych symulacji tego typu struktur. Zaproponowana technika wykorzystuje metodę elementów skończonych (MES) oraz symulacje dynamiki układów wieloczłonowych (MBD). Metoda elementów skończonych dostarcza informacji odnośnie zachowania konstrukcji w stanie rozwiniętym, podczas gdy analiza dynamiki układu wieloczłonowego daje informacje dotyczące zachowania układu podczas realizacji różnych scenariuszy rozwijania, wyboru aktywnych cięgien, wartości samonapężenia oraz rozkładu sił w elementach podczas rozwijania. Połączenie MES i MBD daje możliwość dokładnych i niezawodnych symulacji skomplikowanych struktur do jakich należą rozwijalne konstrukcje tensegrity.

Opisana metoda zaprezentowana jest na przykładzie rozwijalnego słupa tensegrity, który bazuje na popularnym module tensegrity – *simplex* trójzastrzałowym. Analiza słupa przy wykorzystaniu proponowanej techniki dowodzi jej przydatności do wykonywania złożonych symulacji dynamicznych struktur rozwijalnych.

Analizowany słupek składa się z czterech modułów *simplex* połączonych w węzłach poprzez wspólne ciągną podstaw. Wykorzystano moduły prawo- i lewoskrętne ustawione naprzemiennie. W pracy rozpatrywano trzy konfiguracje słupa: standardowy (4.00 m), wysoki (4.15 m) i niski (3.75 m). Są to w rzeczywistości trzy warianty tego samego słupa, ponieważ górny moduł może być rozwinięty do różnej wysokości, zależnie od rozpatrywanego zastosowania. Wszystkie moduły *simplex* mają taką samą długość zastrzałów, a dostosowanie wysokości odbywa się poprzez zmianę długości cięgien.

Stosując opisaną technikę, można analizować rozmaite zmiany geometrii i zmiany właściwości fizycznych struktur tensegrity. Przeprowadzone symulacje pozwalają na zbadanie pracy konstrukcji zarówno pod względem jakościowym jak i ilościowym. W pracy przeanalizowano dwa schematy rozwijania słupa w celu określenia liczby i wyboru aktywnych cięgien: schemat A (rozwijanie pionowe) i schemat B (rozwijanie poziome). Analiza schematu B – konfiguracji, która zakłada wstępny montaż indywidualnych modułów w pozycji poziomej, a następnie rozwijanie modułu po module – dała obiecujące wyniki z punktu widzenia fizycznej realizacji. Struktura taka mogłaby zostać zbudowana z powszechnie dostępnych materiałów, z wykorzystaniem standardowych siłowników.

Przeprowadzone symulacje dowiodły, że proponowana technika jest wydajna pod względem czasu i kosztów obliczeń. Ma duży potencjał do stosowania w analizie skomplikowanych systemów tensegrity zarówno podczas fazy rozwijania jak i w stanie rozwiniętym, bez konieczności wykonywania kosztownych i długotrwałych badań laboratoryjnych.

Received: 23.06.2020, Revised: 17.08.2020